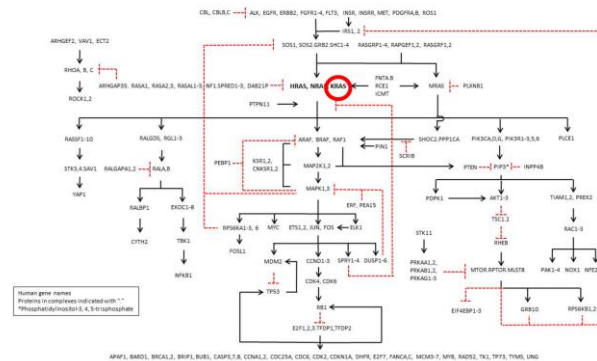


- Identify compounds that bind directly to KRAS or prevent it activating its immediate effectors

The Ras Pathway 2.0



- Molecular description of interaction between KRAS, RAF1 and the plasma membrane
 - Collaboration with the NCI, Dept of Energy, 4 National Labs

Uncovering a membrane-distal conformation of KRAS available to recruit RAF to the plasma membrane

Que N. Van^a, Cesar A. López^b, Marco Tonelli^c, Troy Taylor^a, Ben Niu^{d,1}, Christopher B. Stanley^e, Debsindhu Bhowmik^e, Timothy H. Tran^a, Peter H. Frank^a, Simon Messing^a, Patrick Alexander^a, Daniel Scott^{f,2}, Xiaoying Ye^{a,2}, Matt Drew^a, Oleg Chertov^a, Mathias Lösche^{f,g,h}, Arvind Ramanathanⁱ, Michael L. Gross^d, Nicolas W. Hengartner^b, William M. Westler^c, John L. Markley^c, Dhirendra K. Simanshu^a, Dwight V. Nissley^a, William K. Gillette^a, Dominic Esposito^a, Frank McCormick^{a,3}, S. Gnanakaran^b, Frank Heinrich^{g,h}, and Andrew G. Stephen^{a,3}

^aNational Cancer Institute RAS Initiative, Cancer Research Technology Program, Frederick National Laboratory for Cancer Research, Leidos Biomedical Research, Inc., Frederick, MD 21702; ^bTheoretical Biology and Biophysics Group, Los Alamos National Laboratory, Los Alamos, NM 87545; ^cNational Magnetic Resonance Facility at Madison, Biochemistry Department, University of Wisconsin–Madison, Madison, WI 53706; ^dNational Mass Spectrometry Resource, Department of Chemistry, Washington University in St. Louis, St. Louis, MO 63130; ^eComputational Sciences and Engineering Division, Oak Ridge National Laboratory, Oak Ridge, TN 37831; ^fDepartment of Biomedical Engineering, Carnegie Mellon University, Pittsburgh, PA 15213; ^gDepartment of Physics, Carnegie Mellon University, Pittsburgh, PA 15213; ^hCenter for Neutron Research, National Institute of Standards and Technology, Gaithersburg, MD 20899; and ⁱData Science and Learning Division, Argonne National Laboratory, Lemont, IL 60439

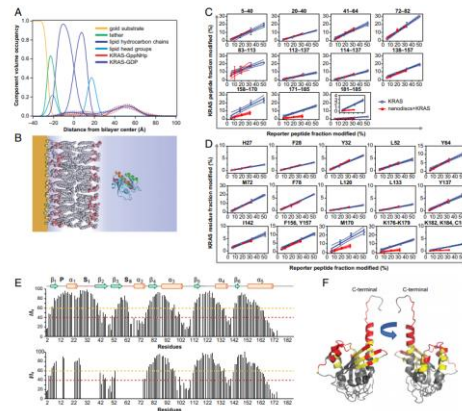


Fig. 1. NR, POPC, and NMR data of membrane-bound KRAS. (A) NR-derived CVO profiles of KRAS-GppNHp and KRAS-GppNpp associated with 70:30 POPC:POPS stBLM. The membrane structure shown is from the measurement of KRAS-GppNHp. The KRAS-GDP profile was added to match that of KRAS-GppNHp in surface coverage. (B) Cartoons of the stBLM-associated KRAS-GppNHp G-domain at a membrane distance in quantitative agreement with the NR results. The orientation of the rotationally reoriented G-domain cannot be determined from the NR data, and an exemplary orientation is shown. Helices of orange ribbon, α 1 (green ribbon), and α 2 (red ribbon) are highlighted for reference. (C) POPC dose-response curves for various regions of KRAS-GDP as represented by peptides from proteolysis of unlabeled (blue) and nanobody-bound (red) protein. The nanobody concentration was varied to change the vertical axis to the protein (or the time provided for reaction). Data for each region are plotted as the fraction modified of the representative peptide α , the fraction modified by peptides from proteolysis of unlabeled (blue) and nanobody-bound (red) protein. Memory-dependent confidence intervals for each curve are shown as shaded regions. (D) Residue-level POPC response curves for nanobody-bound and unlabeled KRAS as determined by MDR analysis of the peptides. (E) NMR PRE ratios for KRAS-GDP (Flag) KRAS-GppNHp (Shikonin) on 70:30 POPC:POPS membranes. Unassigned and excluded residues within the G-domain (2–170) are left blank, see SI Appendix for further information. Secondary structure elements are based on predictions from TALOS-N using backbone chemical shifts. (F) NMR PRE ratios (Hz) from KRAS-GDP projected onto a model structure at 40% (red) and 60% (yellow) cutoffs.

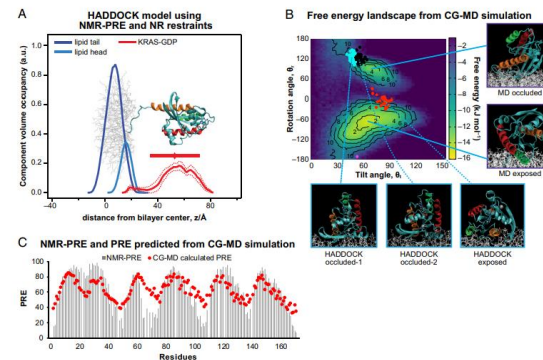


Fig. 2. Correspondence between experimental results and HADDOCK docking and CG MD simulation results of membrane-bound KRAS. (A) CVO profiles of the outer membrane monolayer leaflet and KRAS-GDP derived from HADDOCK with restraints and averaged over the 200 final structures. A representative structure is superimposed. A set of restraints favored G-domain orientations consistent with the NMR PRE results and another, using the R_{eff} (radius of gyration) feature in HADDOCK, approximated the distance of the G-domain from the membrane as determined by NR (indicated by the horizontal line with symbol for peak width and maximum, respectively). (B) Free energy landscape for membrane-bound KRAS that recapitulates the dynamics on a 70:30 POPC:POPS membrane obtained from MARTINI CG MD simulations. The tilt and rotation angles of KRAS with respect to the membrane (16) are based on 10 independent simulation replicas with a combined length of 1 ms. HADDOCK results (using only NMR PRE restraints) in the same coordinate system are overlaid as red, black, magenta, and cyan dots. Insets here show averaged conformations for HADDOCK and CG MD-derived structures. Helices are colored as described in the Fig. 1 legend. (C) Bar plot of measured NMR PRE ratios for KRAS, overlaid with predictions (red dots) for the PRE effect from CG MD simulations for a mixture of 45% occluded and 55% exposed states and an offset distance of 0.45 nm.

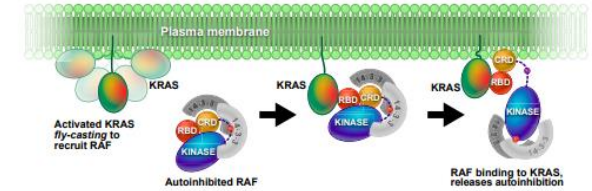


Fig. 5. Model of directional KRAS fly-casting, with the G-domain as bait for the RAF1-RBD, as a mechanism to recruit RAF to the membrane. Membrane-bound KRAS is dynamic, and both membrane-bound and membrane-tethered conformations coexist in fast dynamic exchange. Once freed from a transient, orientationally well-defined membrane-bound state, the KRAS G-domain, while firmly bound to the bilayer through its HVR, is dislodged from the surface under, at least approximate, conservation of the orientation defined by the membrane contact. This dynamic process facilitates the capture of the large effector protein which would not efficiently bind the small GTPase buried in the membrane. The autoinhibited RAF is modeled after a cryo-EM structure (10) in which the CRD is sequestered and the RBD, at the periphery of the RAF14-3-3 complex, is available for interaction with KRAS.

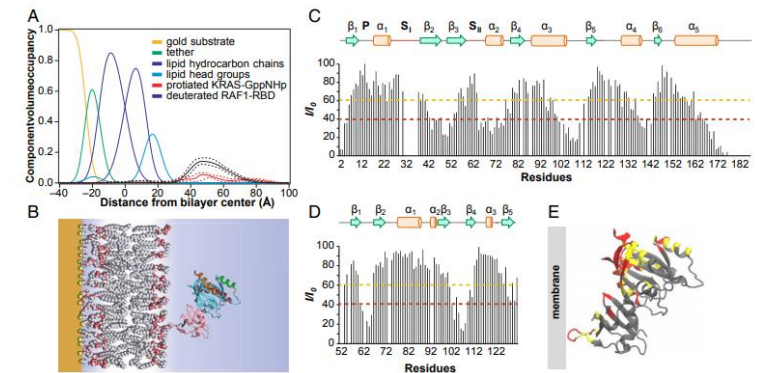


Fig. 3. NR and NMR data orient KRAS-GppNHp/RAF1-RBD on a membrane. (A) NR-derived CVO profiles of the KRAS-GppNHp/RAF1-RBD complex bound to an stBLM composed of 70:30 POPC:POPS. (B) Cartoons of the stBLM and the protein obtained by rigid-body modeling with the complex crystal structure (PDB 6VJJ). (C) and (D) NMR-PRE intensity ratios of ¹⁵N-KRAS/RAF1-RBD and KRAS/¹⁵N-RAF1-RBD in the presence of Gd³⁺-labeled POPC:POPS nanodiscs, respectively. Unassigned and excluded residues within the G-domain (2–170) and RBD are left blank, see SI Appendix for further information. (E) NMR-PREs mapped onto the fitted structure in B using 40% (red) and 60% (yellow) cutoffs.

ARTICLE *Biophysics* *Computational Biology*

Machine Learning-driven Multiscale Modeling Reveals Lipid-Dependent Dynamics of RAS Signaling Proteins

- › Helgi Ingolfsson, Chris Neale, Timothy Carpenter, Rebika Shrestha, Cesar Lopez, Timothy Tran, Tomas Opperstrup, Harsh Bhatia, Liam Stanton, Xiaohua Zhang, Shiv Sundram, Francesco Di Natale, Animesh Agarwal, Gautham Dharuman, Sara Kokkila Schumacher, Thomas Turbyville, Gulcin Gulden, Que Van, Debanjan Goswami, Frantz Jean-Francios, Constance Agamasu, De Chen, Jeevapani Hettige, Timothy Travers, Sumantra Sarkar, Michael Surh, Yue Yang, Adam Moody, Shusen Liu, Brian Van Essen, Arthur Voter, Arvind Ramanathan, Nicolas Hengartner, Dharendra Simanshu, Andrew Stephen, Peer-Timo Bremer, S Gnanakaran, James Glosli, Felice Lightstone, Frank McCormick, Dwight Nissley, Frederick Streit

NCI RAS Initiative - Resources and interactions

Reagents

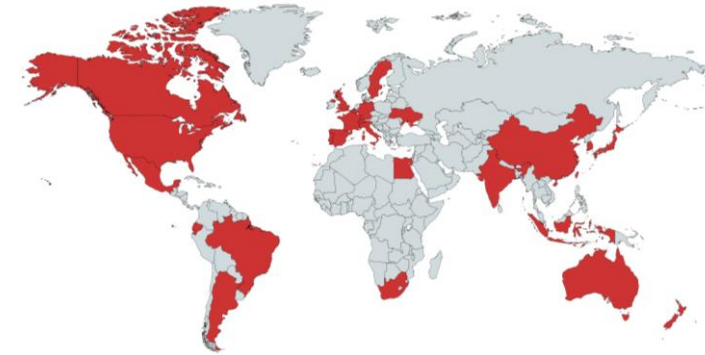
552 Universities and NPOs, 42 states, 42 countries, 6 continents
10,067 plasmids & vectors (through Addgene)

- 1946 individual RAS and RAS pathway plasmids
- At least 1 individual request for each of the 180 genes
- 19 complete RAS pathway kits (360 plasmids each)
- 21 complete RAS mutant kits (61 plasmids each)

820 cell lines

RAS-dependent MEFs licensed to 9 companies

KRAS-FMe materials licensed to 6 companies



Collaborations

27 Academic Institutions

11 Strategic (National Labs, Advocacy, NIH)

10 Industry

Community Outreach and Engagement

2 RAS Symposia (3rd in 2021)

8 RAS Community Workshops

4 AACR/NCI Special Sessions Presentations

Participation in NCI Ras Synthetic Lethality Network

40 publications

cCRADAs

16 cCRADAs - universities, biotechs and pharma

\$11.1 M in funds to FNLCR

- 51 FTE years funded
- 28 in-kind FTE years from collaborator

Recent Publications

The small molecule BI-2852 induces a nonfunctional dimer of KRAS

Timothy H. Tran^a, Patrick Alexander^a, Srisathiyarayanan Dharmaiah^a, Constance Agamasu^a, Dwight V. Nissley^a, Frank McCormick^{a,b}, Dominic Esposito^a, Dhirendra K. Simanshu^a, Andrew G. Stephen^a, and Trent E. Balias^{a,1}

RESEARCH ARTICLE

Atypical KRAS^{G12R} Mutant Is Impaired in PI3K Signaling and Macropinocytosis in Pancreatic Cancer

G. Aaron Hobbs¹, Nicole M. Baker¹, Anne M. Miermont², Ryan D. Thurman³, Mariaelena Pterobon⁴, Timothy H. Tran⁵, Andrew O. Anderson², Andrew M. Waters⁵, J. Nathaniel Diehl⁷, Bjoern Papke⁶, Richard G. Hodge⁶, Jennifer E. Klomp⁶, Craig M. Goodwin⁶, Jonathan M. DeLiberty⁷, Junning Wang⁸, Raymond W.S. Ng⁸, Prson Gautam⁹, Kirsten L. Bryant⁴, Dominic Esposito⁵, Sharon L. Campbell^{1,4}, Emanuel F. Petricoin III⁴, Dhirendra K. Simanshu¹, Andrew J. Aguirre^{8,10}, Brian M. Wolpin⁸, Krister Wennerberg^{9,11}, Udo Rudloff^{2,12}, Adrienne D. Cox^{1,6,13}, and Channing J. Der^{1,6,7}

CANCER RESEARCH | METABOLISM AND CHEMICAL BIOLOGY

Undermining Glutaminolysis Bolsters Chemotherapy While NRF2 Promotes Chemoresistance in KRAS-Driven Pancreatic Cancers

Suman Mukhopadhyay^{1,2}, Debanjan Goswami^{1,2}, Pavan P. Adisheshaiah², William Burgan^{1,2}, Ming Yi^{1,2}, Theresa M. Guerin³, Serguei V. Kozlov³, Dwight V. Nissley^{1,2}, and Frank McCormick^{1,2,4}

Cell Reports



Article

Structural Insights into the SPRED1-Neurofibromin-KRAS Complex and Disruption of SPRED1-Neurofibromin Interaction by Oncogenic EGFR

Wupeng Yan,^{1,4} Evan Markegard,^{2,4} Srisathiyarayanan Dharmaiah,¹ Anatoly Urisman,² Matthew Drew,¹ Dominic Esposito,¹ Klaus Scheffzek,³ Dwight V. Nissley,¹ Frank McCormick,^{1,2,*} and Dhirendra K. Simanshu^{1,5,*}
¹NCI RAS Initiative, Cancer Research Technology Program, Frederick National Laboratory for Cancer Research, Leidos Biomedical Research, Inc., Frederick, MD 21701, USA
²Helen Diller Family Comprehensive Cancer Center, University of California, San Francisco, San Francisco, CA 94158, USA
³Institute of Biological Chemistry, Biocenter, Medical University of Innsbruck, 6020 Innsbruck, Austria
⁴These authors contributed equally
⁵Lead Contact
*Correspondence: dhirendra.simanshu@nlcr.nih.gov (D.K.S.), frank.mccormick@ucsf.edu (F.M.)
<https://doi.org/10.1016/j.celrep.2020.107909>

SCIENTIFIC
REPORTS
nature research



RESEARCH ARTICLE



ssGSEA score-based Ras dependency indexes derived from gene expression data reveal potential Ras addiction mechanisms with possible clinical implications

Ming Yi^{1,2}, Dwight V. Nissley¹, Frank McCormick^{1,2} & Robert M. Stephens^{1,2}

KRAS G13D sensitivity to neurofibromin-mediated GTP hydrolysis

Dana Rabara^{a,1}, Timothy H. Tran^{a,1}, Srisathiyarayanan Dharmaiah^a, Robert M. Stephens^a, Frank McCormick^{a,b,2}, Dhirendra K. Simanshu^{a,2}, and Matthew Holderfield^{a,2,3}

^aNCI RAS Initiative, Cancer Research Technology Program, Frederick National Laboratory for Cancer Research, Frederick, MD 21701; and ^bHelen Diller Family Comprehensive Cancer Center, University of California, San Francisco, San Francisco, CA 94158

Membrane interactions of the globular domain and the hypervariable region of KRAS4b define its unique diffusion behavior

Debanjan Goswami^{1†}, De Chen^{1†}, Yue Yang², Prabhakar R Gudla¹, John Columbus¹, Karen Worthy¹, Megan Rigby¹, Madeline Wheeler¹, Suman Mukhopadhyay¹, Katie Powell¹, William Burgan¹, Vanessa Wall¹, Dominic Esposito¹, Dhirendra K Simanshu¹, Felice C Lightstone², Dwight V Nissley¹, Frank McCormick³, Thomas Turbyville^{1*}

¹NCI RAS Initiative, Cancer Research Technology Program, Frederick National Laboratory for Cancer Research, Frederick, United States; ²Biosciences and Biotechnology Division, Lawrence Livermore National Laboratory, Livermore, United States; ³UCSF Helen Diller Family Comprehensive Cancer Center, School of Medicine, University of California, San Francisco, San Francisco, United States

NCI RAS Initiative – cCRADAs

- Beatson Institute
- Daiichi-Sankyo
- Eli Lilly and Company
- Evotec
- Genomic Institute of the Novartis Research Foundation
- KyRas Therapeutics
- Northeastern University
- Pharma Arava
- Sanofi
- TheRas, Inc
- TOSK, Inc.
- University of California at San Francisco
- University of Maryland Baltimore
- Weizmann Institute



cCRADA with TheRas



Anna Maciag



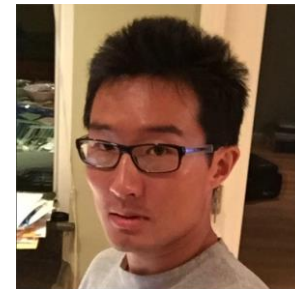
David Turner



Dhirendra Simanshu



Eli Wallace



Yue Yang

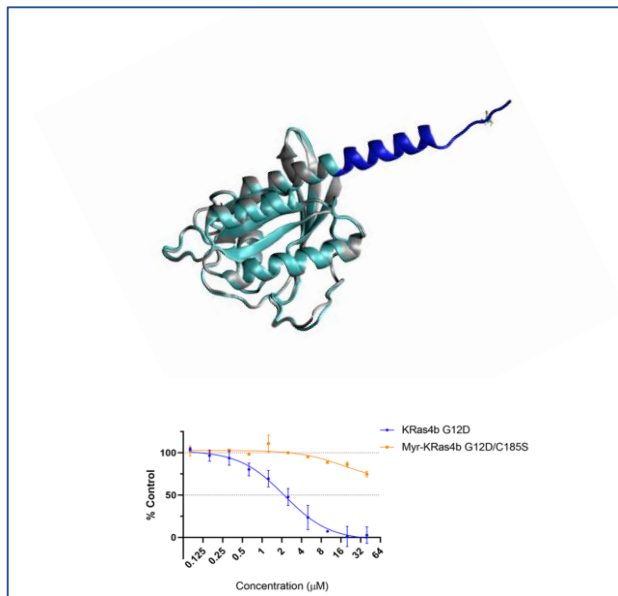


Felice Lightstone

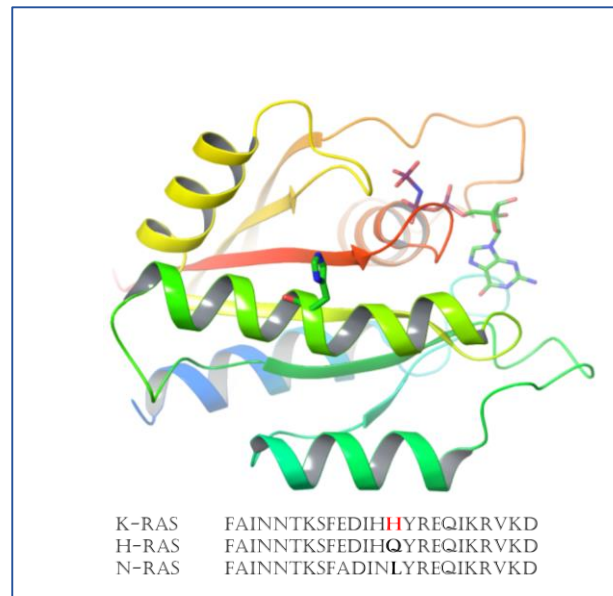


Julian Downward

Preventing KRAS4B processing by blocking C185



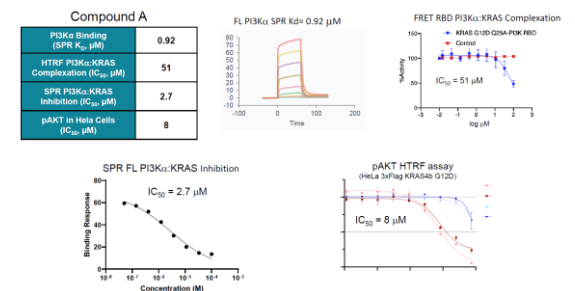
Targeting H95: unique residue on KRAS



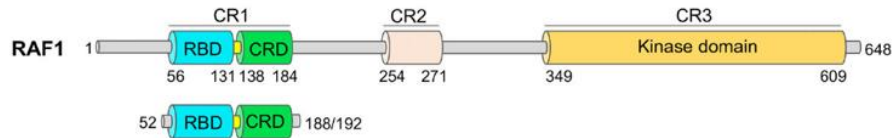
Blocking activation of PI3 kinase by KRAS

Binding of Ras to Phosphoinositide 3-Kinase p110 α Is Required for Ras-Driven Tumorigenesis in Mice

Surbhi Gupta,^{1,4} Antoine R. Ramjaun,^{1,4} Paula Haiko,³ Yihua Wang,¹ Patricia H. Warne,¹ Barbara Nicko,¹ Emma Nye,² Gordon Stamp,² Kari Alitalo,³ and Julian Downward^{1*}
¹Signal Transduction Laboratory
²Experimental Pathology Laboratory
³Cancer Research UK London Research Institute, 44 Lincoln's Inn Fields, London WC2A 3PX, UK
⁴Molecular/Cancer Biology, Biomedicum Helsinki, University of Helsinki, P.O.B. 63 (Haartmaninkatu 8), FIN-00014 Helsinki, Finland
 *These authors contributed equally to this work.
 *Correspondence: downward@cancer.org.uk
 DOI: 10.1016/j.cell.2007.03.051



Targeting Ras-dependent Raf activation



MOLECULAR AND CELLULAR BIOLOGY, Nov. 1998, p. 6698-6710
0270-7306/98/\$04.00+0
Copyright © 1998, American Society for Microbiology. All Rights Reserved.

Vol. 18, No. 11

The RafC1 Cysteine-Rich Domain Contains Multiple Distinct Regulatory Epitopes Which Control Ras-Dependent Raf Activation

MARTINA DAUB,¹ JOHANNES JÖCKEL,¹ THOMAS QUACK,¹ CHRISTOPH K. WEBER,²
FRANK SCHMITZ,¹ ULF R. RAPP,² ALFRED WITTINGHOFFER,¹ AND CHRISTOPH BLOCK^{1*}

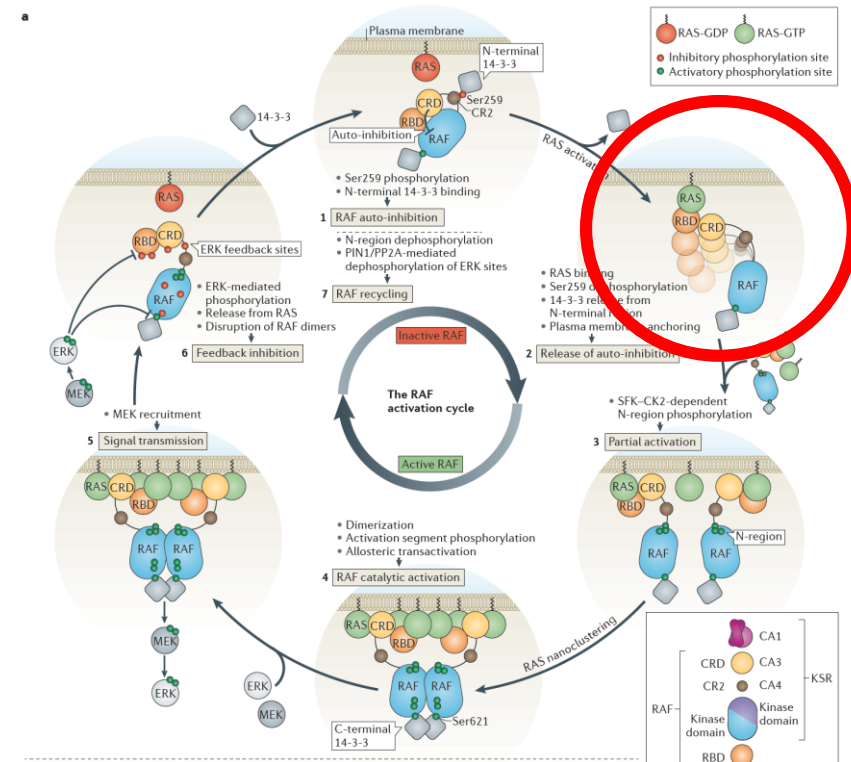
THE JOURNAL OF BIOLOGICAL CHEMISTRY

Vol. 273, No. 34, Issue of August 21, pp. 21578-21584, 1998
Printed in U.S.A.

Identification of Residues in the Cysteine-rich Domain of Raf-1 That Control Ras Binding and Raf-1 Activity*

(Received for publication, March 20, 1998, and in revised form, June 11, 1998)

David G. Winkler^{‡§}, Richard E. Cutler, Jr.^{¶**}, Jonelle K. Drugan^{‡‡§§}, Sharon Campbell^{‡‡§§},
Deborah K. Morrison^{¶**}, and Jonathan A. Cooper^{‡¶¶}

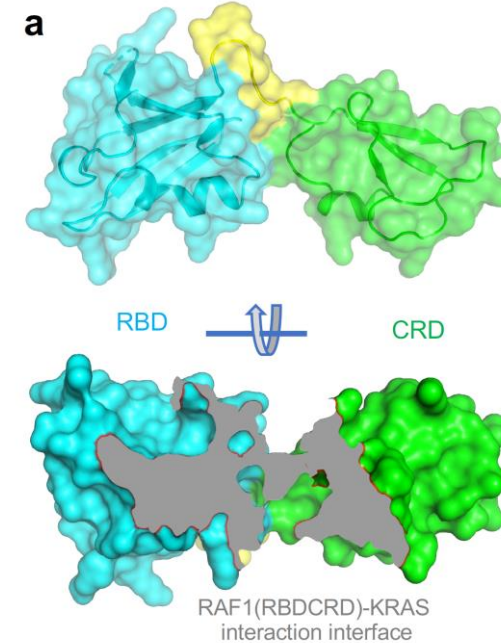
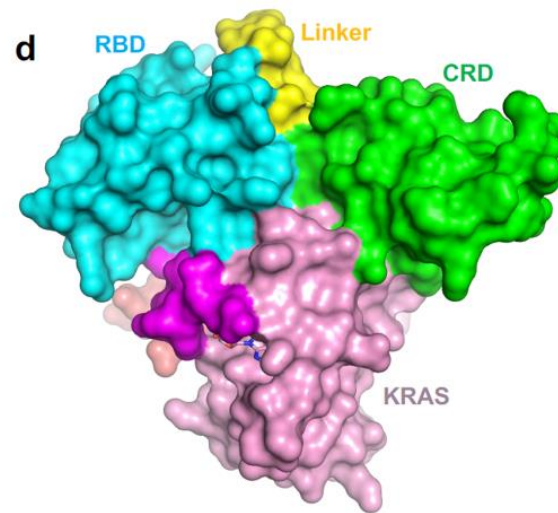
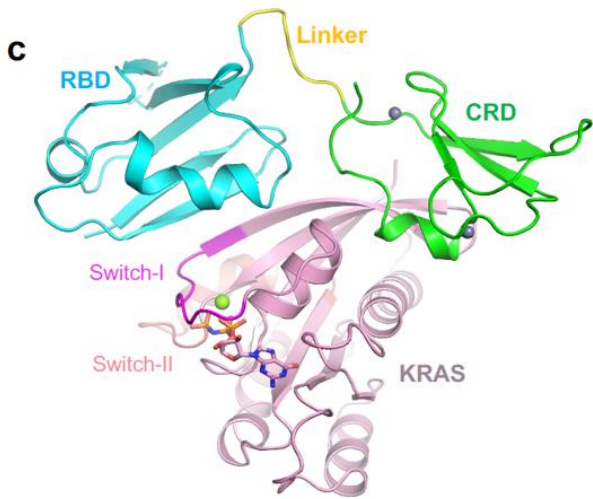
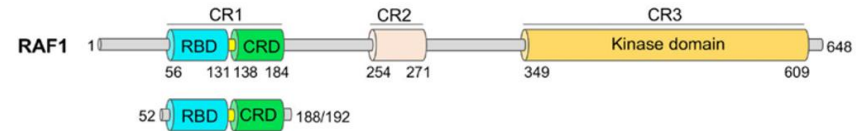


Mutation K144A R164A or K144A L160A did not interfere with Ras binding significantly but did inhibit Raf activation,


Regulation of RAF protein kinases in ERK signalling

Hugo Lavoie¹ and Marc Therrien^{1,2}

First crystal structure of the Raf1 RBD-CRD domain



KRAS interaction with RAF1 RAS-binding domain and cysteine-rich domain provides insights into RAS-mediated RAF activation

Timothy H. Tran, Albert H. Chan, Lucy C. Young, Lakshman Bindu, Chris Neale, Simon Messing, Srisathiyarayanan Dharmiah, Troy Taylor, John-Paul Denson, Dominic Esposito, Dwight V. Nissley, Andrew G. Stephen, Frank McCormick,  Dharendra K. Simanshu

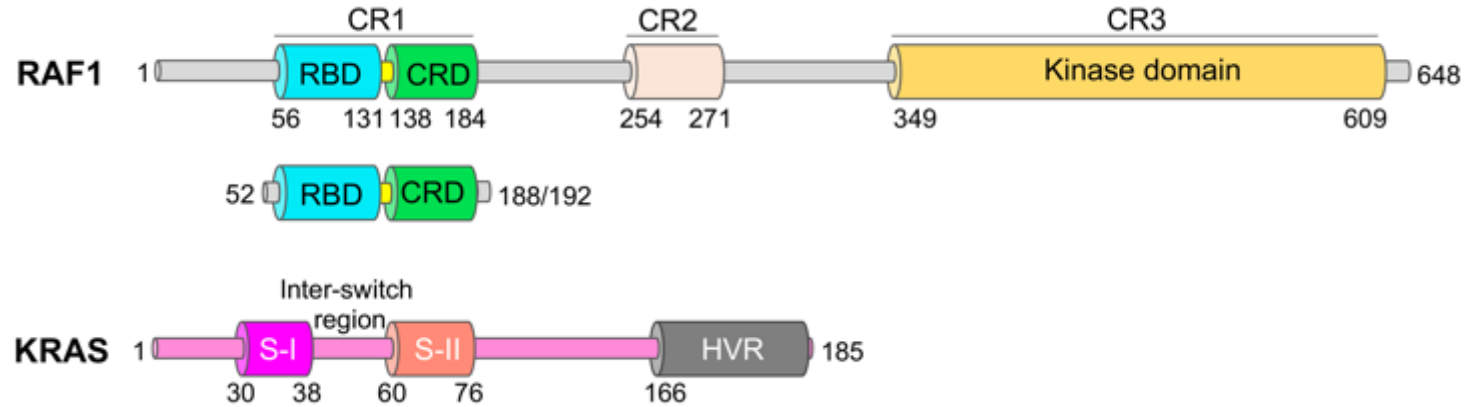


Simanshu

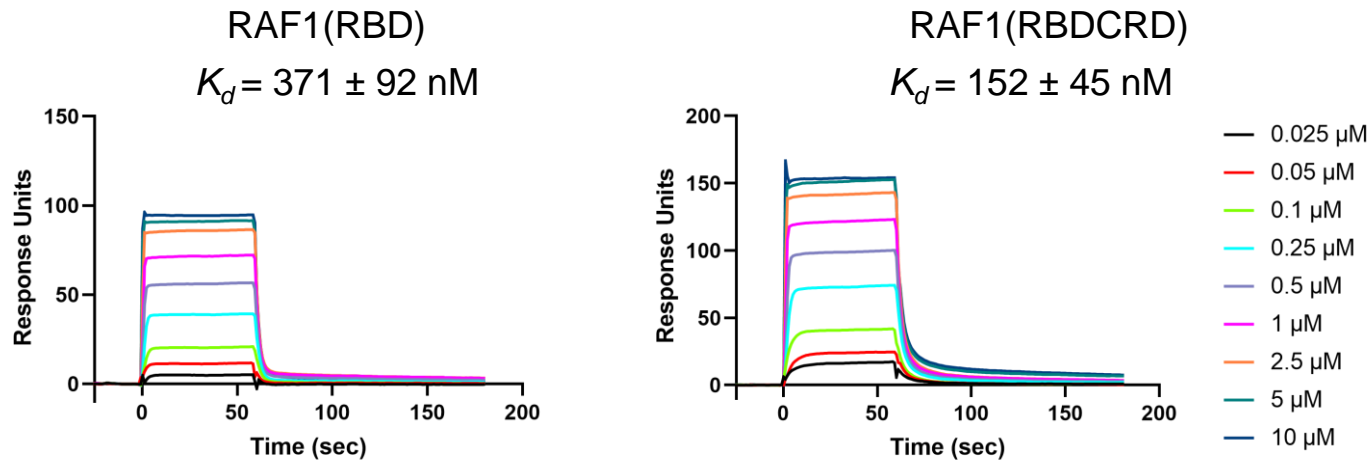


Tim Tran

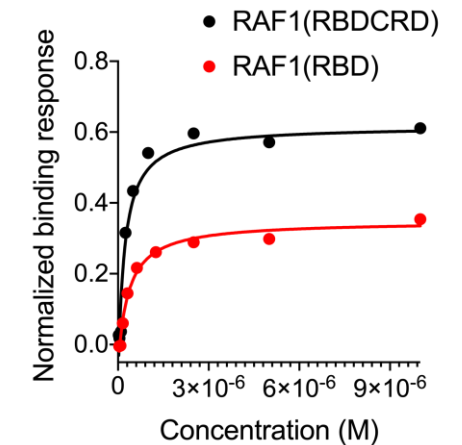
KRAS-RAF1(RBDCRD) complex and SPR analysis



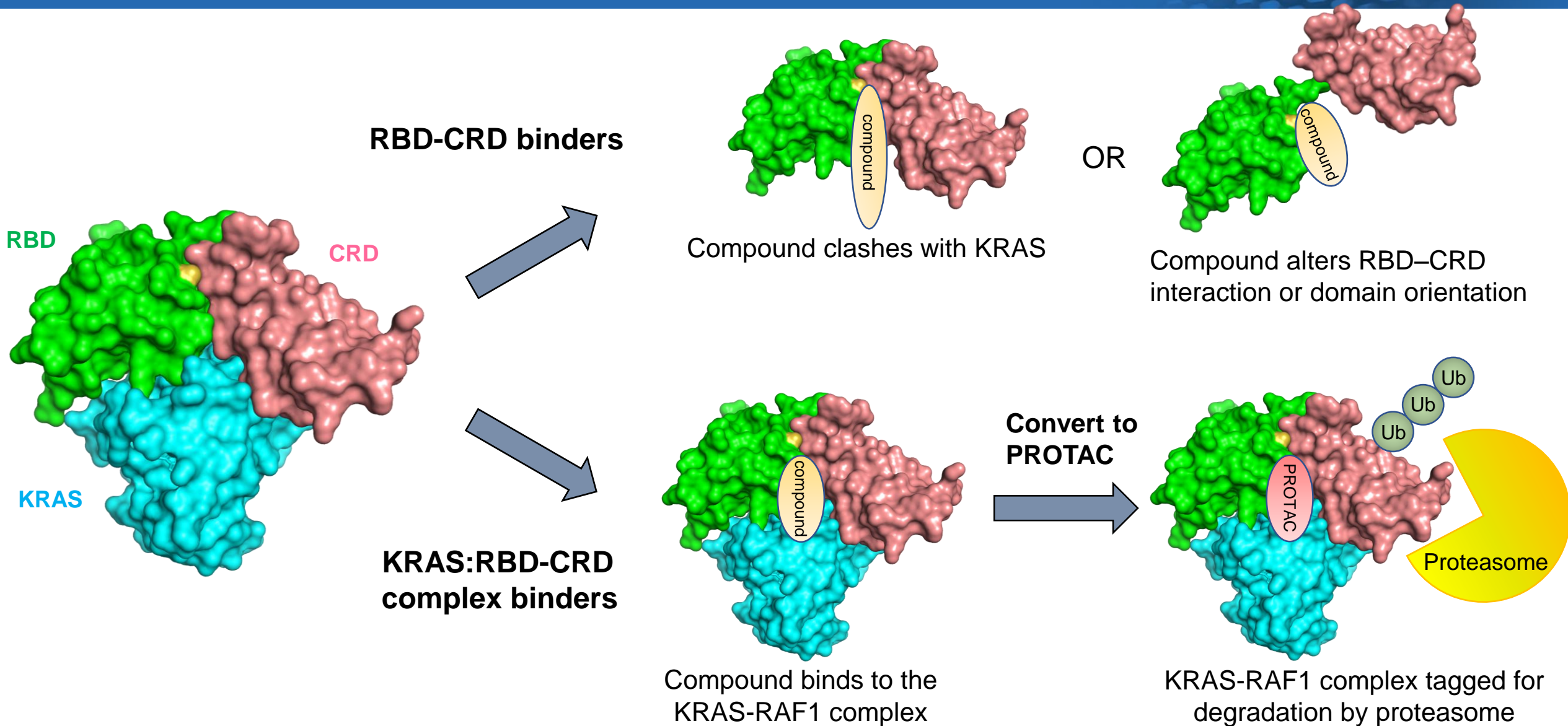
SPR sensorgrams showing the binding of RAF1(RBD) and RAF1(RBDCRD) to KRAS



Steady-state binding isotherms derived from the SPR data



Developing RAF1(RBD-CRD) inhibitors



Sanofi cCRADA : Targeting KRAS-RAF1 (RBD CRD) interaction

CRADA executed in April, 2020

- **Screening strategies:**

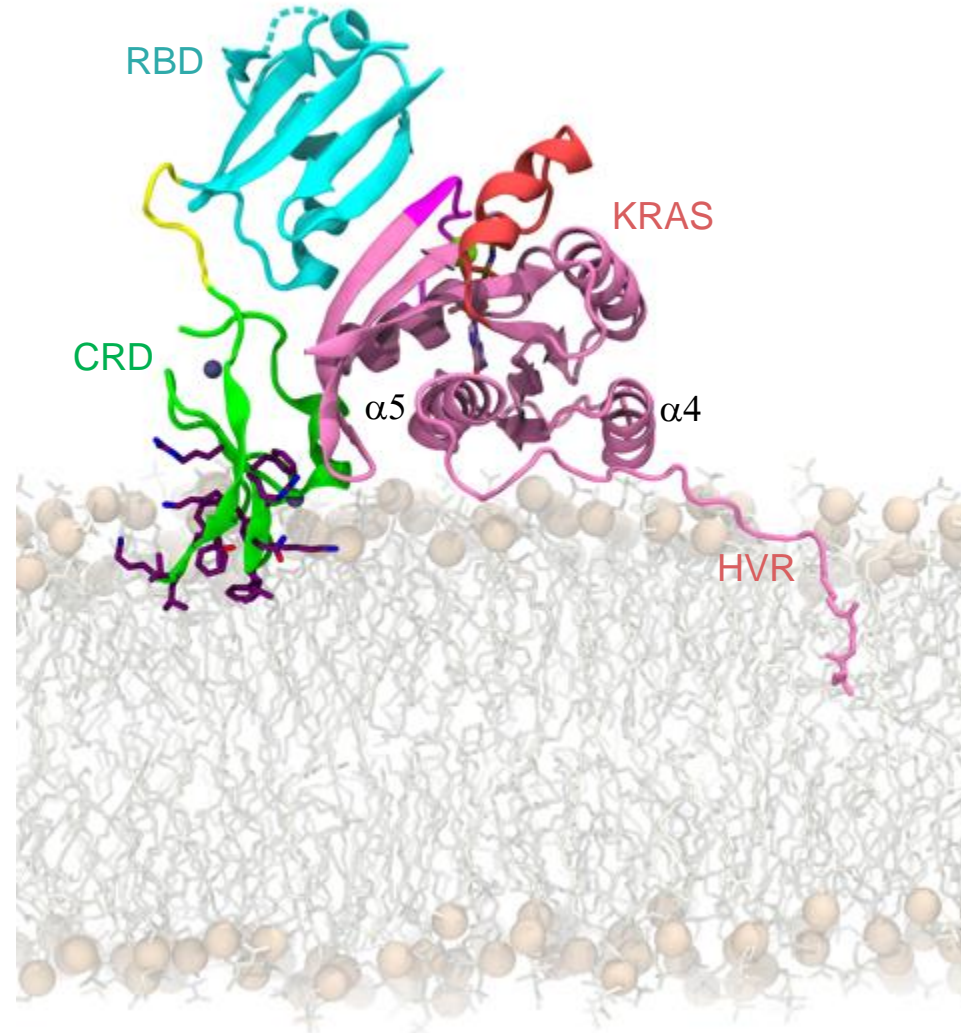
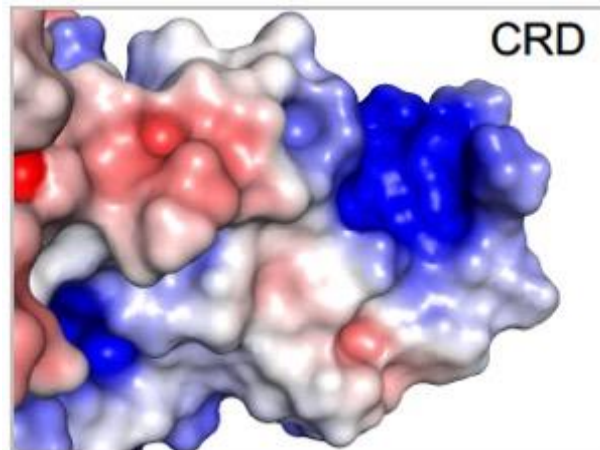
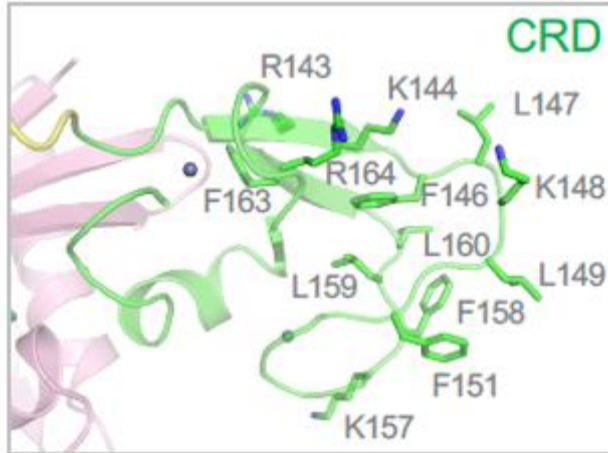
- 19F NMR-fragment screening using Sanofi fragment library
- In silico screening using Sanofi small-molecule library
- DNA encoded library screening (covalent/non-covalent)
- HTS screen using Sanofi small-molecule library
- MTS SEC based Affinity Selection Mass Spectrometry screen

Screening completed.
Compound synthesis/ hit validation.

Assay optimization.

Model showing the crystal structure of KRAS-RBDCRD at the membrane

Membrane interacting residues in CRD

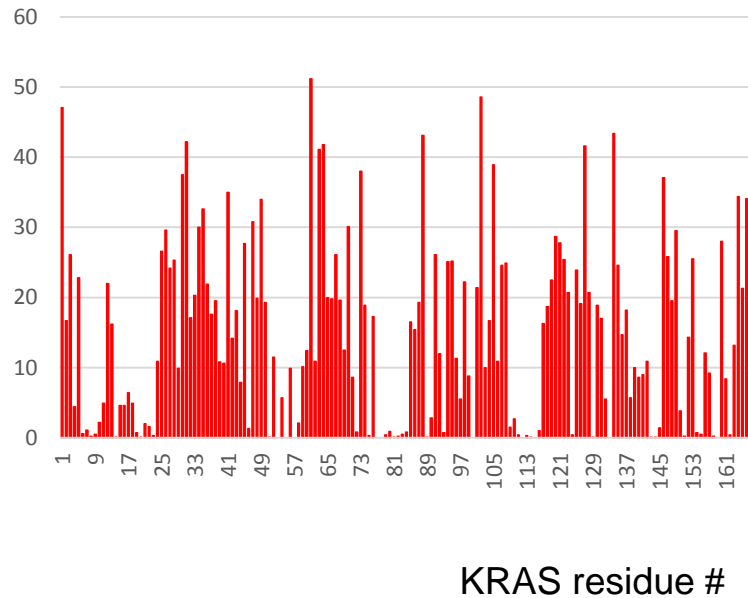


KRAS cysteine surface mutagenesis library

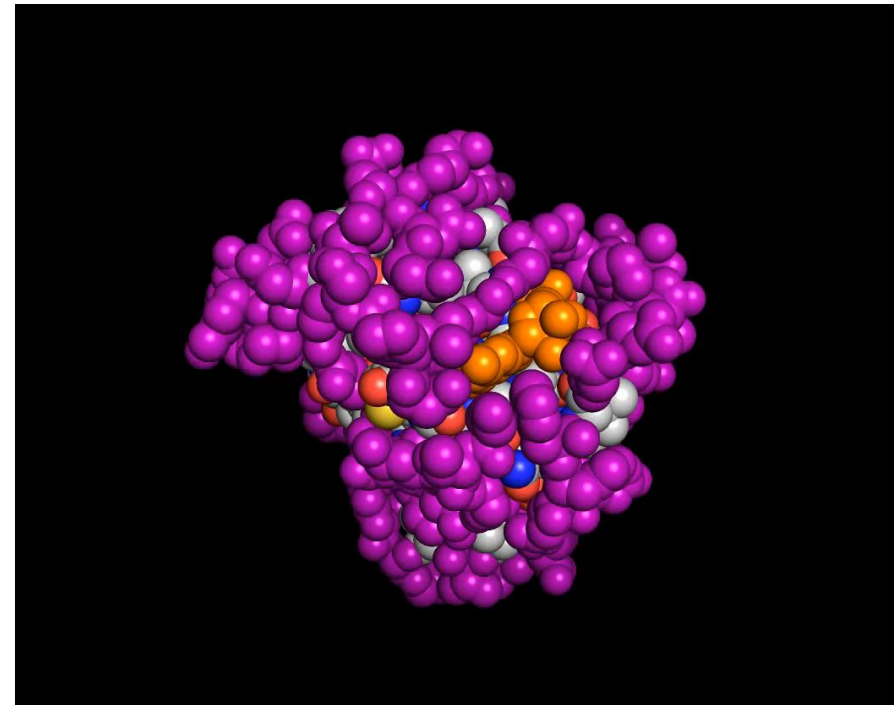


Dom Esposito

Surface accessibility

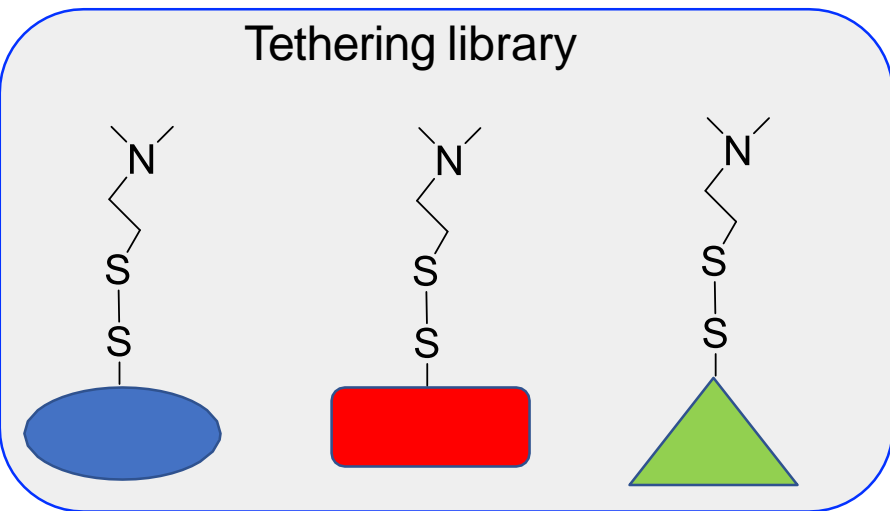


MTEYKLVVVGADGVGKSALTIQLIQNHFVDEYDP
TIEDSYRKQVVIDGETCLLDILDTAGQEEYSAMR
DQYMRTGEGFLCVFAINNTKSFEDIHHYREQIKR
VKDSSEVPMVLVGNKSDLPSRTVDTKQAQDLARS
YGIPFIETSAKTRQGVDDAFYTLVREIRKHKEK



95 residues

Tethering can identify fragment binding pockets adjacent to cysteines

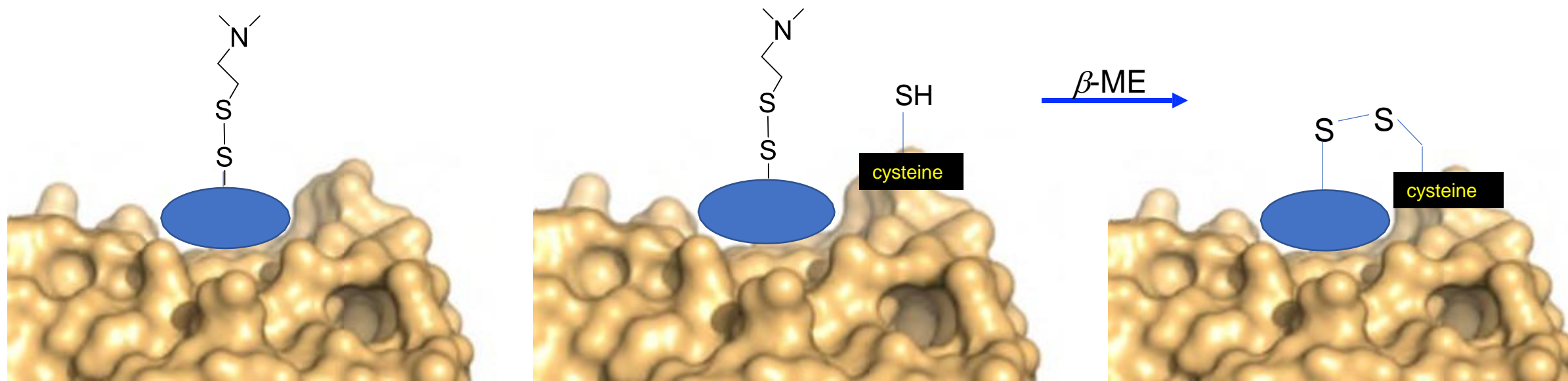


TETHERING: Fragment-Based Drug Discovery

Daniel A. Erlanson, James A. Wells,
and Andrew C. Braisted

*Sunesis Pharmaceuticals, Inc., 341 Oyster Point Boulevard, South San Francisco,
California 94080; email: erlanson@sunesis.com; jaw@sunesis.com*

Erlanson DA, Wells JA, Braisted AC. Tethering: fragment-based drug discovery.
Annu Rev Biophys Biomol Struct. 2004;33:199-223.



FNL disulfide tethering library

- >2000 high quality and chemically diverse fragments
- Good fragment-like properties
 - MW <300
 - ClogP ≤ 3
 - Number of hydrogen bond donors/acceptors ≤ 3
- Minimize overly complex molecules
- Minimize unnecessary stereochemistry
- Exclusion of PAINS / reactive groups
- Current library of 1163 compounds stored as 50 mM DMSO stocks

Parameter	Range
Molecular weight	80 - 343
Heavy atoms	5 - 21
Chiral centers	0 - 2
HB donors	0 - 2
HB acceptors	0 - 5
Rotatable bonds	0 - 4
Polar surface area	< 106 Å ²



Anna Maciag

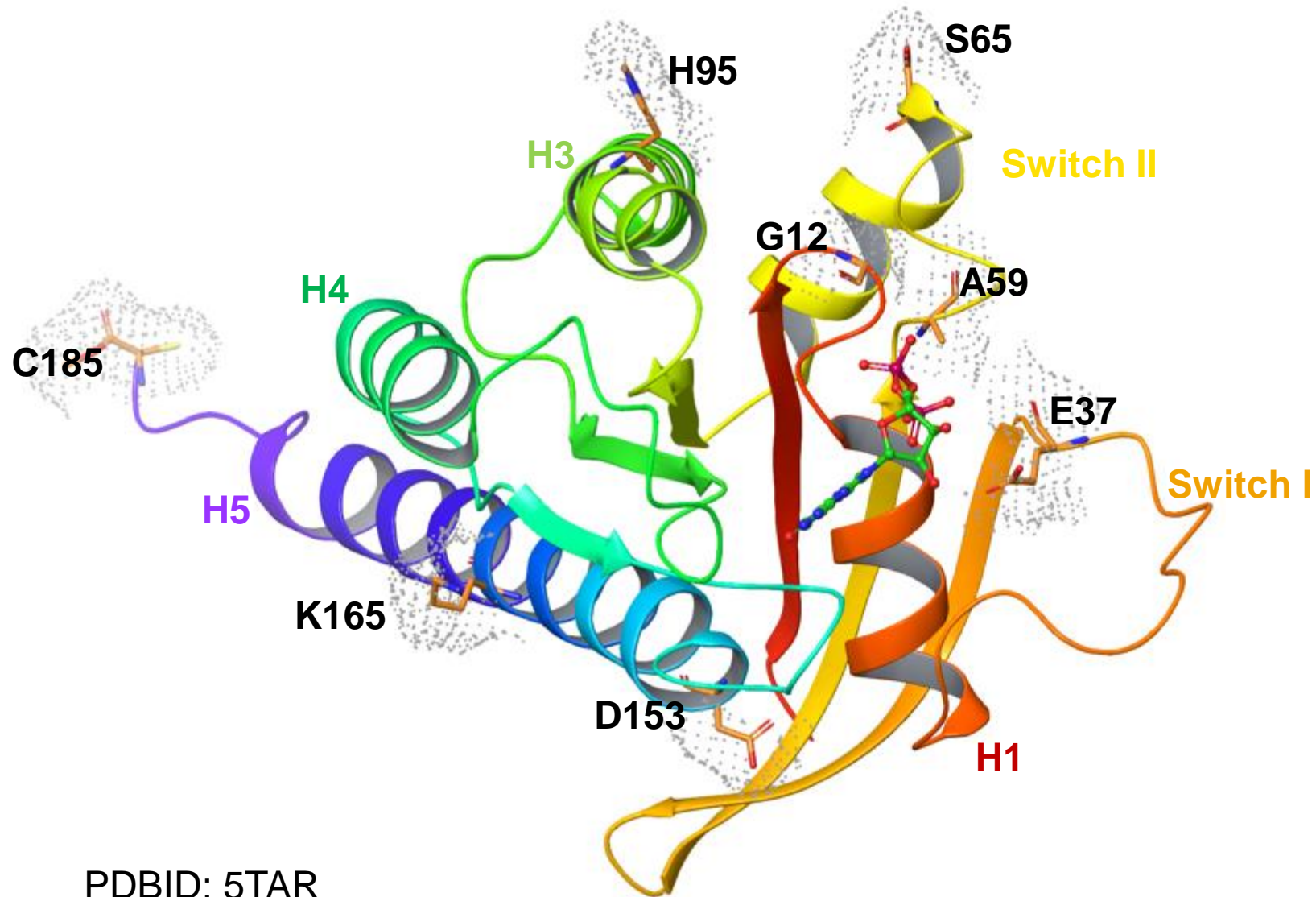


David Turner



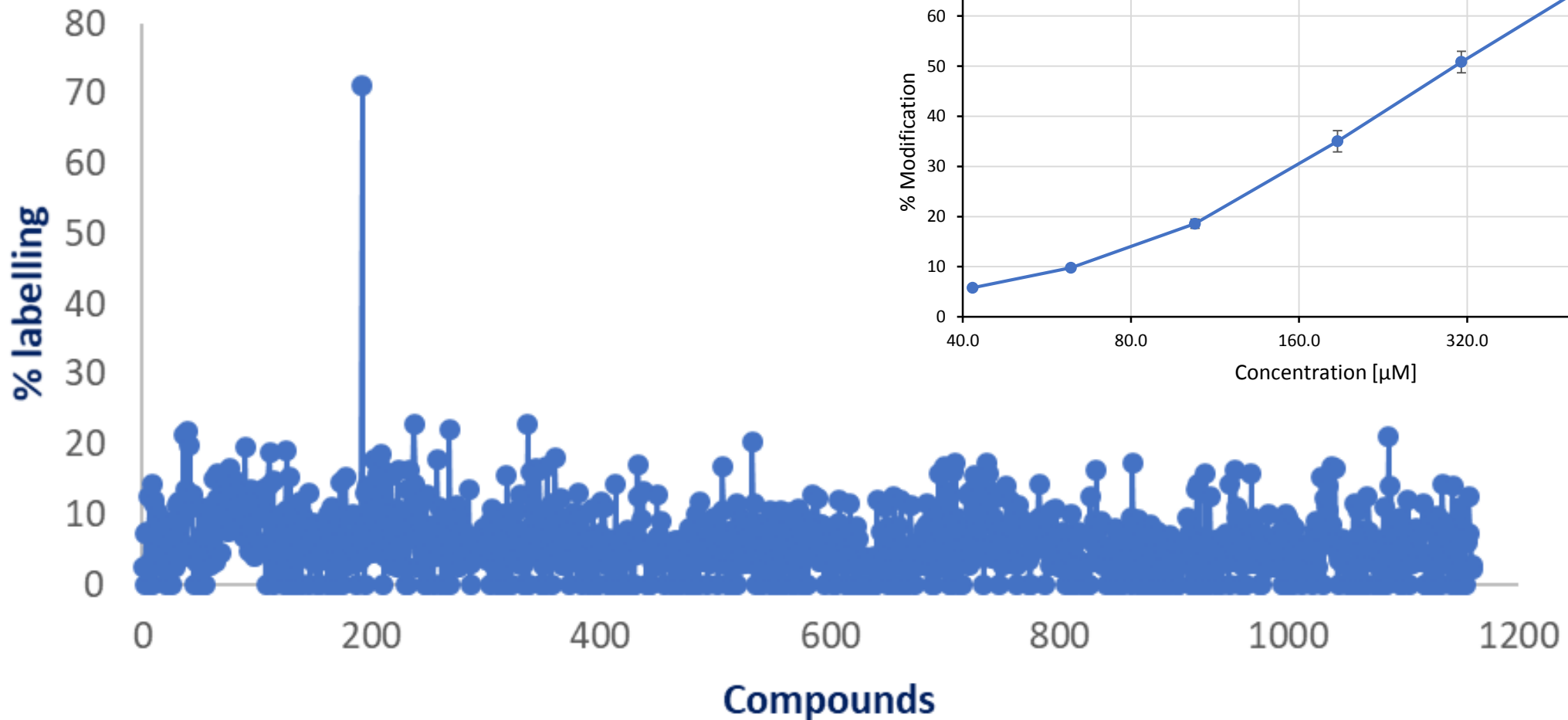
Vandana Kumari

Completed screens: residue mapping

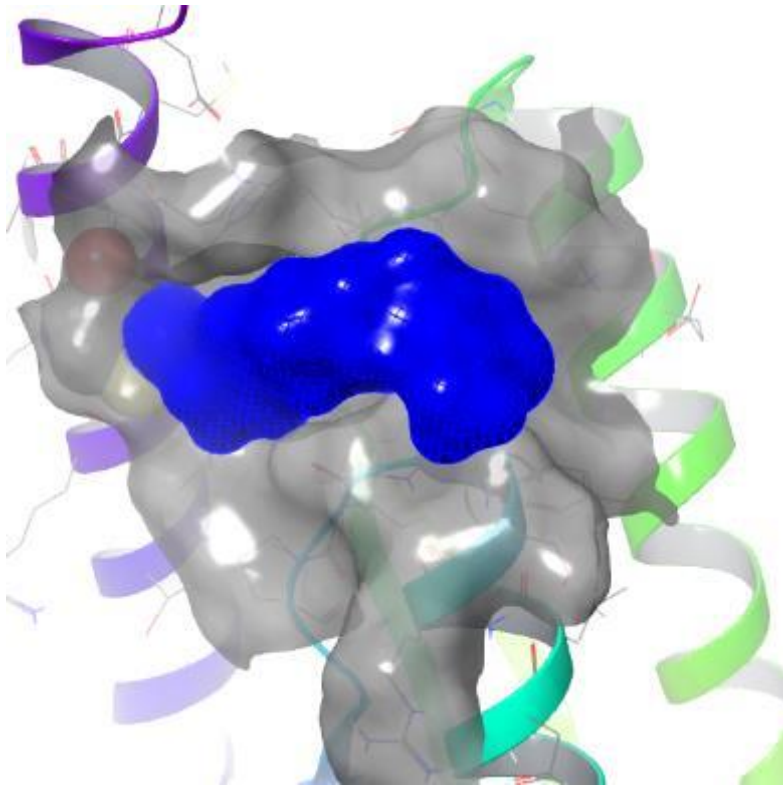


PDBID: 5TAR

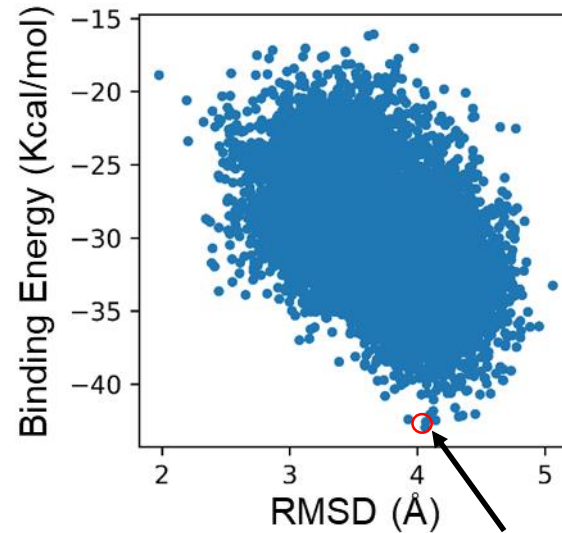
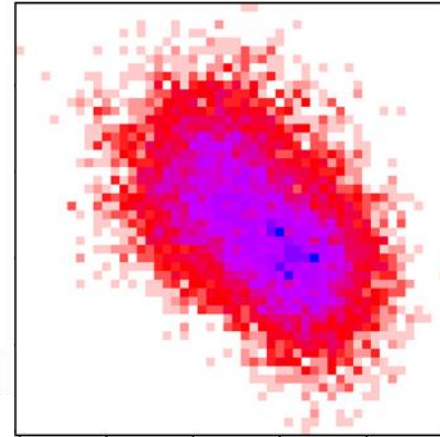
Tethering screen: KRAS G12C/C118S (GppNHp)



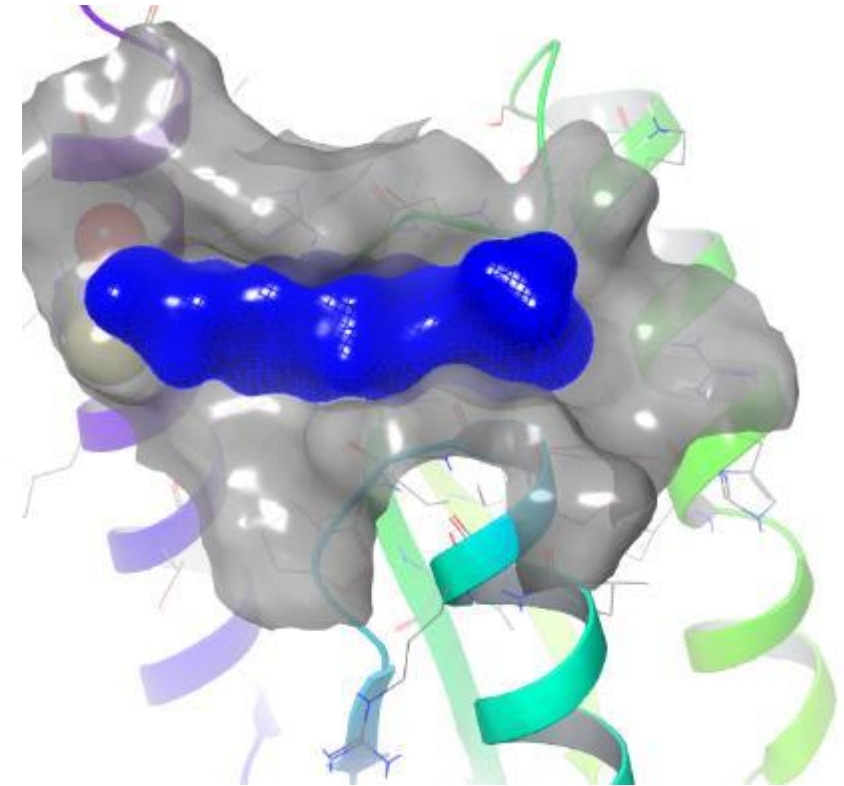
Best pose observed during MD simulations



Starting pose
(covalently docked pose to a
crystal structure)



Best energy



Best pose

Best pose from all MD simulations
MM-GBSA binding energies : -42.94 kcal/mol

Goals and approaches

Goals:

- Hit optimizations with limited binding pocket/structural information
- Discovery of new pockets not detectable in crystal structures-
identification of cryptic pockets

Approaches:

- Computer aided drug design
 - Molecular docking for pose prediction (starting point for simulations)
 - Molecular dynamics (MD) simulations for pose refinement
 - Enhanced MD for cryptic pocket identifications

- Thanks!